HIGH POWER HEATING AND PROPAGATION USING FAST MAGNETOSONIC WAVES IN THE WISCONSIN TOKAPOLE II

(Presented at the 1979 IEEE International Conference on Plasma Science, June 4-6, 1979, Varennes, Québec, Canada)

A.P. Biddle
J.C. Sprott

PLP 800

June 1979

Plasma Studies

University of Wisconsin

Past measurements were made with the MKI antenna, which consisted of a 1/8" × 1" × 6" strip of copper which viewed the plasma through a 1/2" thick Macor window. This assembly was mounted in a pump port located on the bottom of the machine. While useful for propagation measurements, it was actually very inefficient at coupling energy to the plasma via the fast mode. The thick evanescent region between the antenna and plasma resulted in very poor coupling, as most of the energy was reflected back to be deposited on the walls. Figure 1 shows that for our densities and a typical mode number of 7, the evanescent length is about 8 cm. This is comparable to the plasma to antenna spacing. As heating goes as $|E|^2$, this gave a maximum power transfer of ~ 15% of input power.

Experimental evidence is shown in Fig. 2. This shows the ion saturation current, roughly proportional to density, and the drive current to the oscillator, which is monotonous though not linear to increased plasma loading. Since the plasma forms initially near the edge[1] and is then carried inward as the discharge progresses, the loading for the MKI antenna also peaked early in time, and then decreased. Installation of a limiter sharply dropped the initial heavy loading, while leaving the mature discharge unaffected.

To improve coupling, a new, insertable MKII antenna was fabricated. Shown in Figure 3, it is similar electrically to the MKI, but is insertable into the tank. It is encased in a Macor block, though it currently has no Faraday shield. Figure 4 shows the marked impovement in loading characteristics. Loading now is constant during the entire discharge. Figure 5 gives the normalized loading with different antenna spacings. The loading is relatively constant over a range of several centimeters, as the increased coupling competes with the limiter action of the antenna.

Since most of the data concerning actual heating was performed in a short period of time, there is considerable room at various interpretations. Figure 6 shows the increase in ion temperature measured by Doppler broadening at the C III 4647 Å line. The quick saturation at OT_i is probably due to saturation of the loss cones which should be especially bad in our machine due to the very small toroidal plasma current. Another possibility is that the impurity dopant may be decoupling from the majority protons. This occurs when the equilibration time between the two species is near the ion energy confinement time. More data needs to be taken, but the same OT_i measured by both HE II and C III lines, which have different equilibtation times, argue against this.

Perhaps the most perplexing aspect is shown in Figs. 7 and 8. There appears to be no dependence on either plasma loading or heating with changes in the toroidal field. This may imply significant loading by electrostatic modes. A Faraday screen is being added. Figure 9 shows a disturbing dependence of impurity radiation on applied RF power. This effect may be simply edge heating, or hopefully is the result energetic ions impacting a dirty machine. Fig. 10 shows a sharp increase in soft x-ray emission. This is probably a result of a combination of electron heating and the increase ion and electron concentrations caused by impurity influx.

REFERENCES

[1]R. Groebner and R. Dexter in "Conference Record-Abstracts, 1979 IEEE International Conference on Plasma Science, June 4-6, 1979, Université de Montréal, Canada."

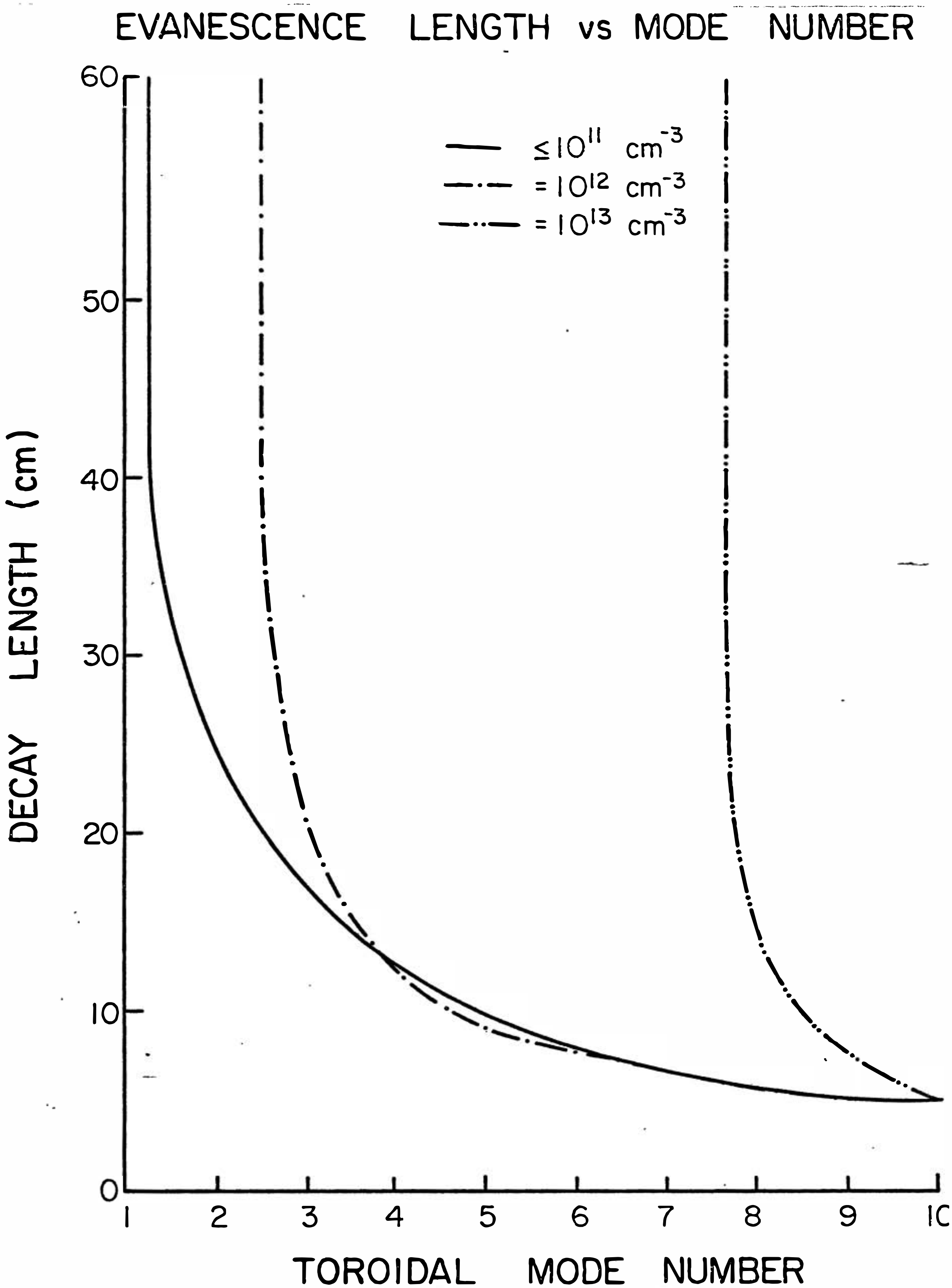
EVANESCENCE LENGTH vs MODE NUMBER
$\leq 10^{11}$ cm^{-3}
$= 10^{12}$ cm^{-3}
$= 10^{13}$ cm^{-3}
DECAY LENGTH (cm)
60
50
40
30
20
10
0
1
2
3
4
5
6
7
8
9
10
TOROIDAL MODE NUMBER

Figure 1

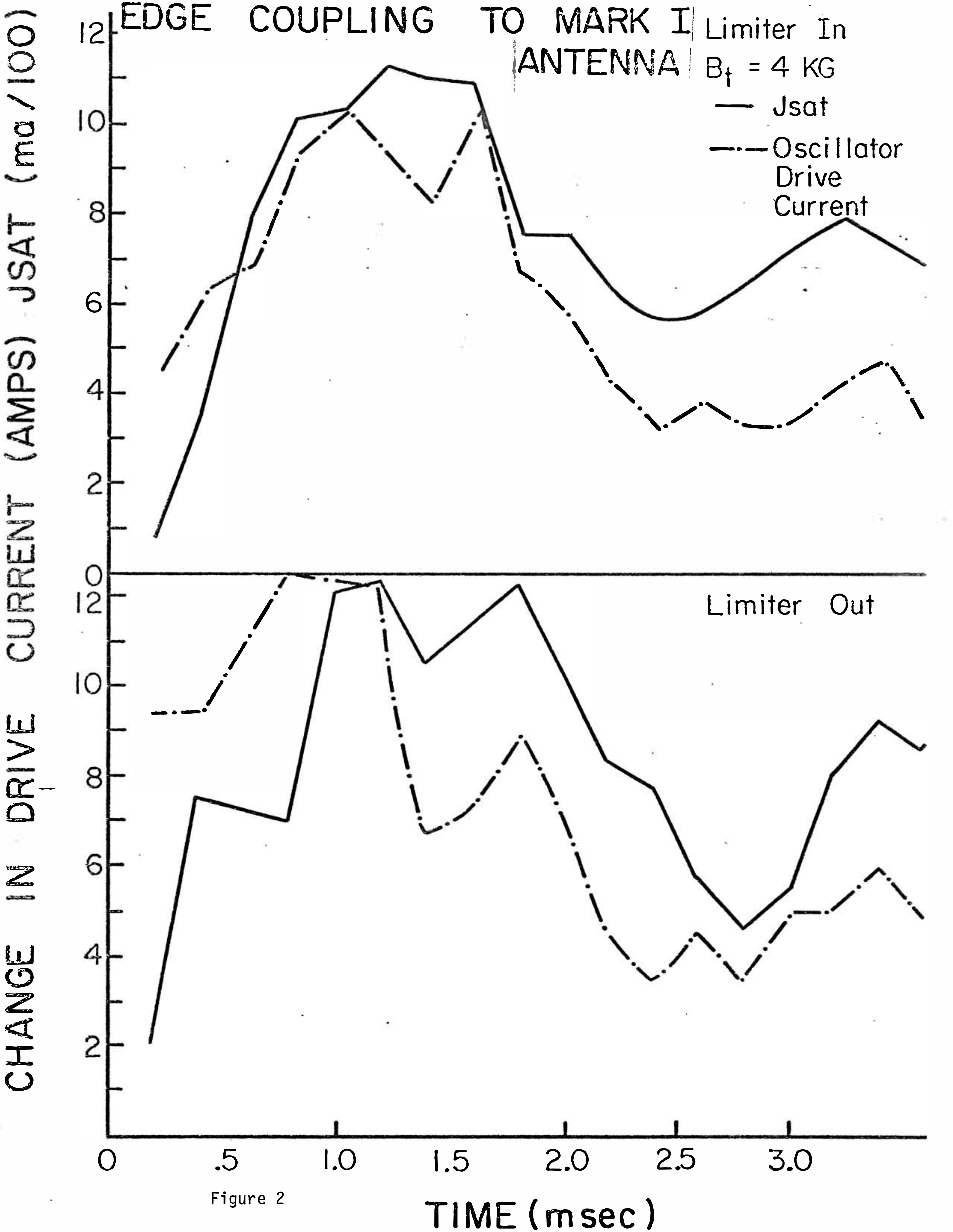
EDGE COUPLING TO MARK I ANTENNA
Limiter In
B_t = 4 KG
Jsat
Oscillator Drive Current
Limiter Out
CHANGE IN DRIVE CURRENT (AMPS) JSAT (ma/100)
TIME (msec)
0
2
4
6
8
10
12
.5
1.0
1.5
2.0
2.5
3.0

Figure 2

TOKAPOLE II FLUX PLOT AND INSERTED ANTENNA

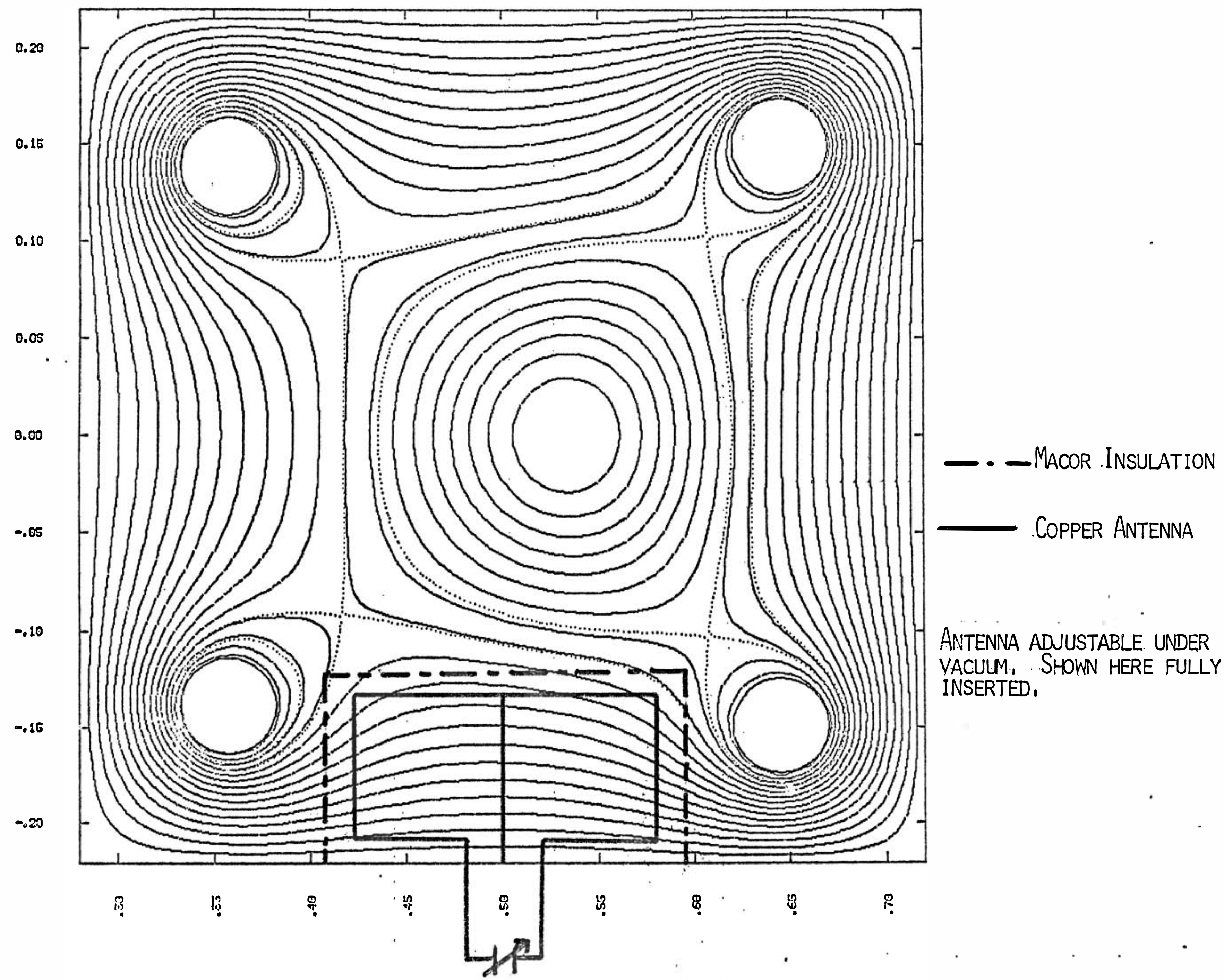

Figure 3

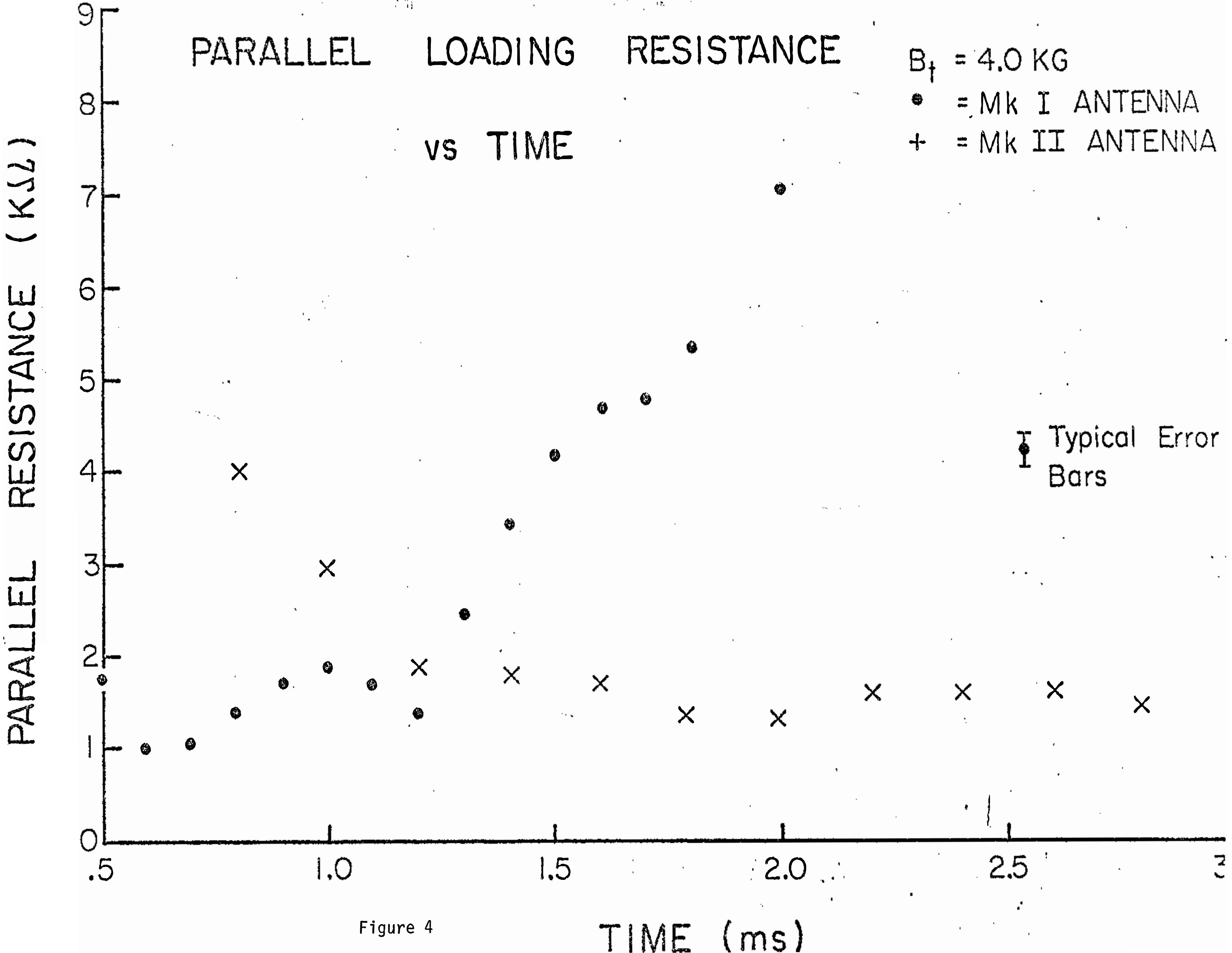
PARALLEL LOADING RESISTANCE
vs TIME
B_t = 4.0 KG
● = Mk I ANTENNA
+ = Mk II ANTENNA
Typical Error Bars
PARALLEL RESISTANCE (KΩ)
0
1
2
3
4
5
6
7
8
9
.5
1.0
1.5
2.0
2.5
3
TIME (ms)

Figure 4

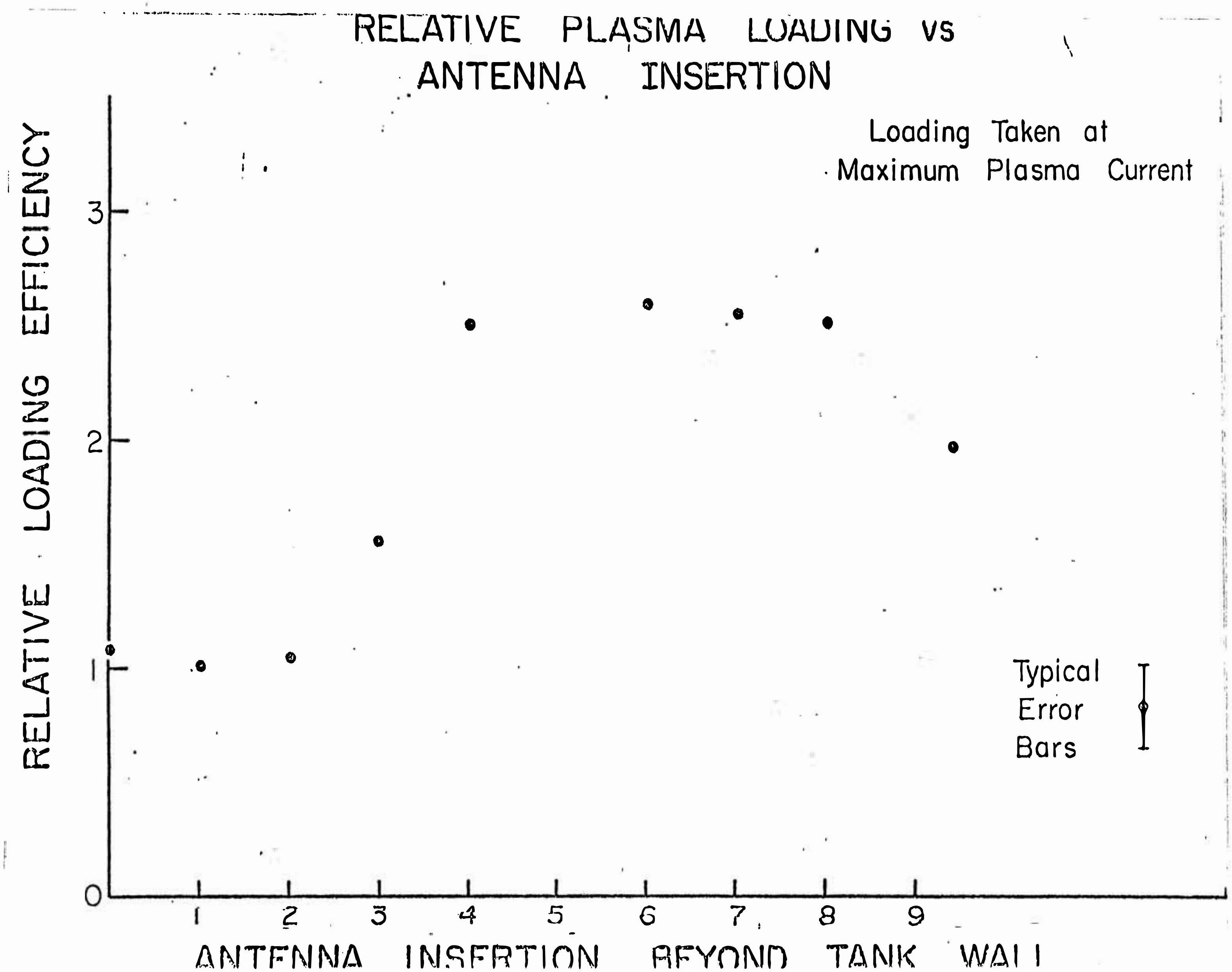
RELATIVE PLASMA LOADING vs
ANTENNA INSERTION
Loading Taken at
Maximum Plasma Current
RELATIVE LOADING EFFICIENCY
3
2
1
0
1
2
3
4
5
6
7
8
9
Typical
Error
Bars
ANTENNA INSERTION BEYOND TANK WALL
Figure 5

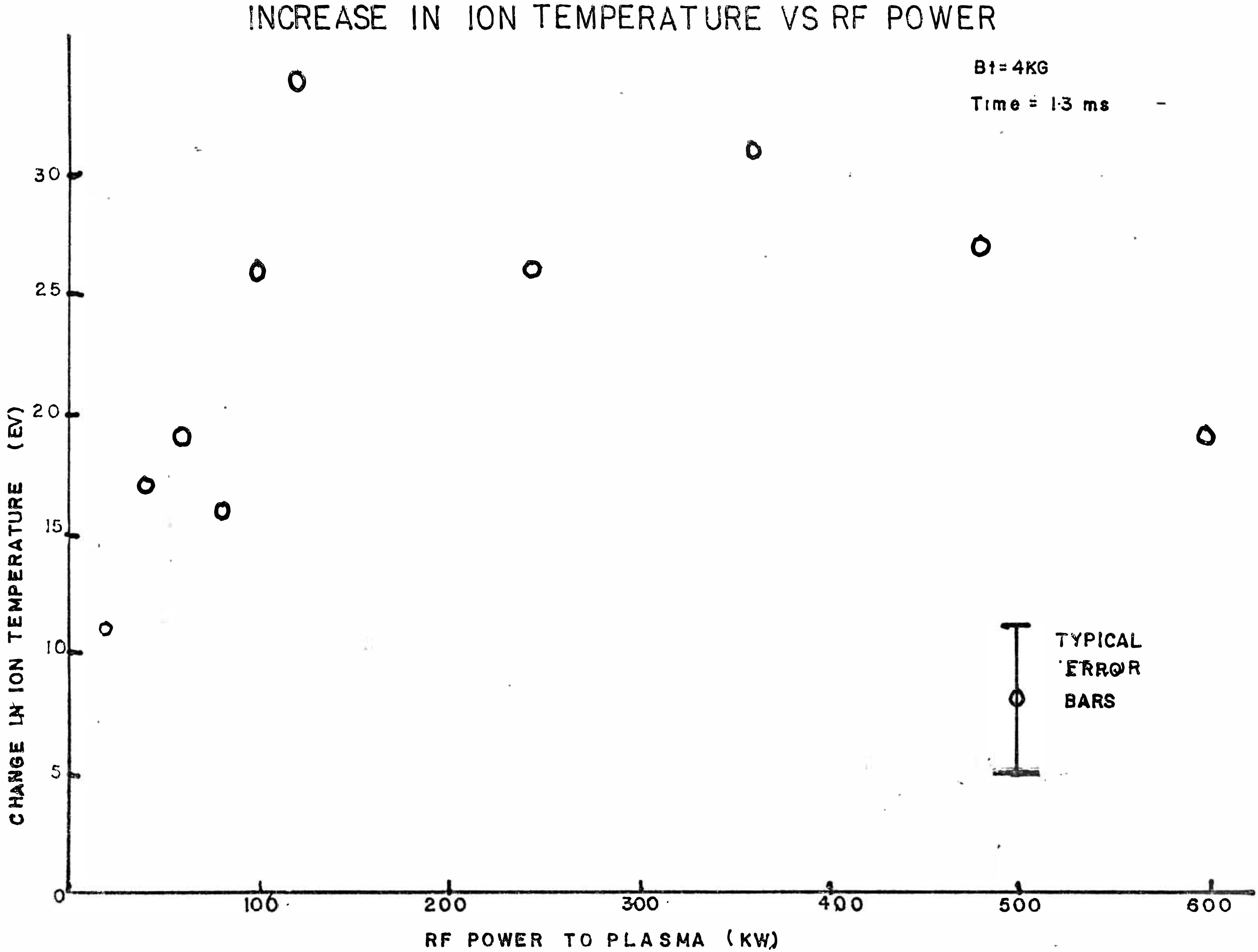
INCREASE IN ION TEMPERATURE VS RF POWER
Bt = 4KG
Time = 1·3 ms
30
25
20
15
10
5
0
CHANGE IN ION TEMPERATURE (EV)
TYPICAL ERROR BARS
100
200
300
400
500
600
RF POWER TO PLASMA (KW)
Figure 6

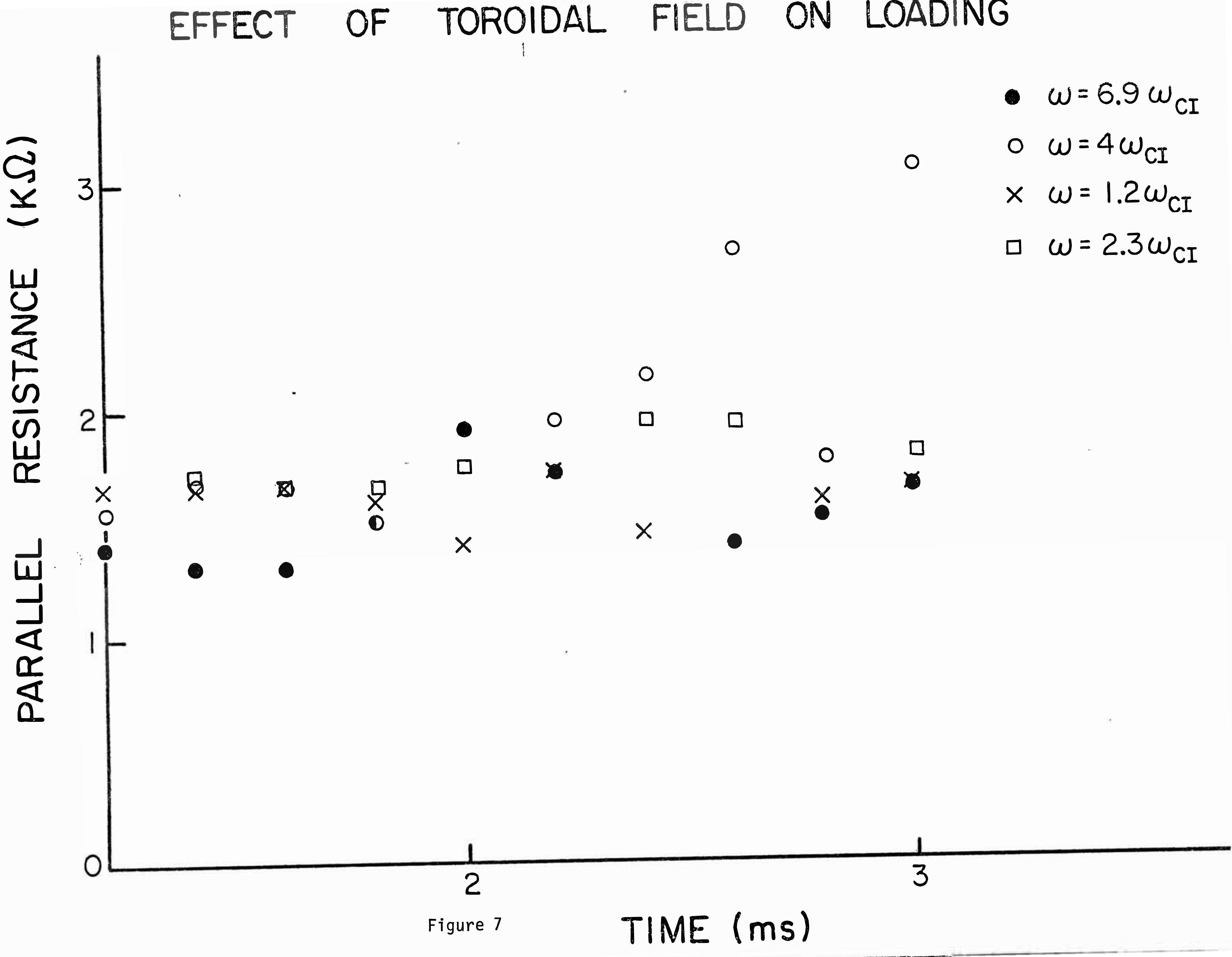

EFFECT OF TOROIDAL FIELD ON LOADING
PARALLEL RESISTANCE (KΩ)
TIME (ms)
0
1
2
3
2
3
$\omega = 6.9\,\omega_{CI}$
$\omega = 4\,\omega_{CI}$
$\omega = 1.2\,\omega_{CI}$
$\omega = 2.3\,\omega_{CI}$

Figure 7

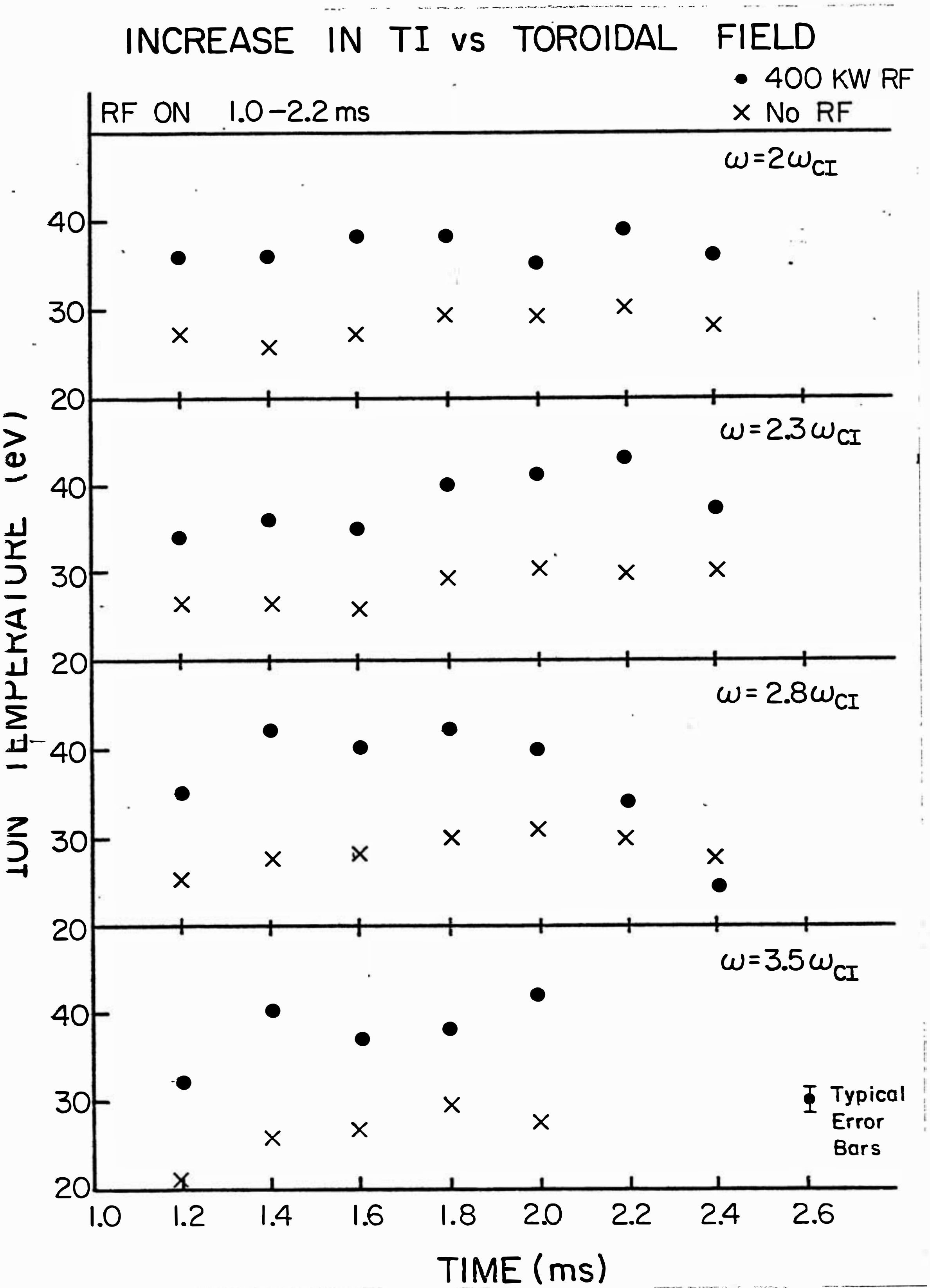
INCREASE IN TI vs TOROIDAL FIELD
• 400 KW RF
× No RF
RF ON 1.0–2.2 ms
ω=2ω_CI
ω=2.3ω_CI
ω=2.8ω_CI
ω=3.5ω_CI
ION TEMPERATURE (eV)
20
30
40
Typical Error Bars
1.0
1.2
1.4
1.6
1.8
2.0
2.2
2.4
2.6
TIME (ms)

Figure 8

CIII VS APPLIED RF POWER

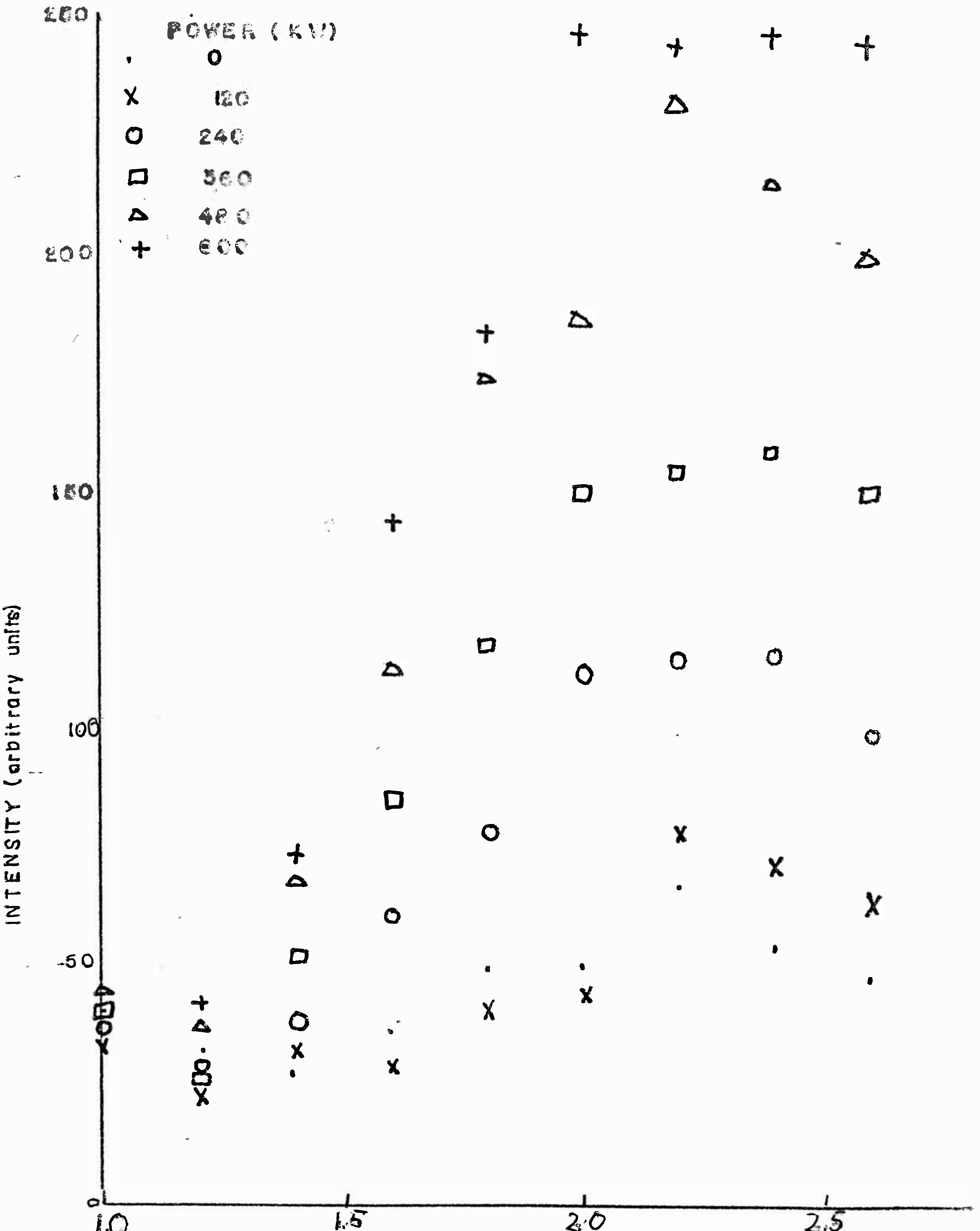

Figure 9

SOFT X-RAY EMISSION

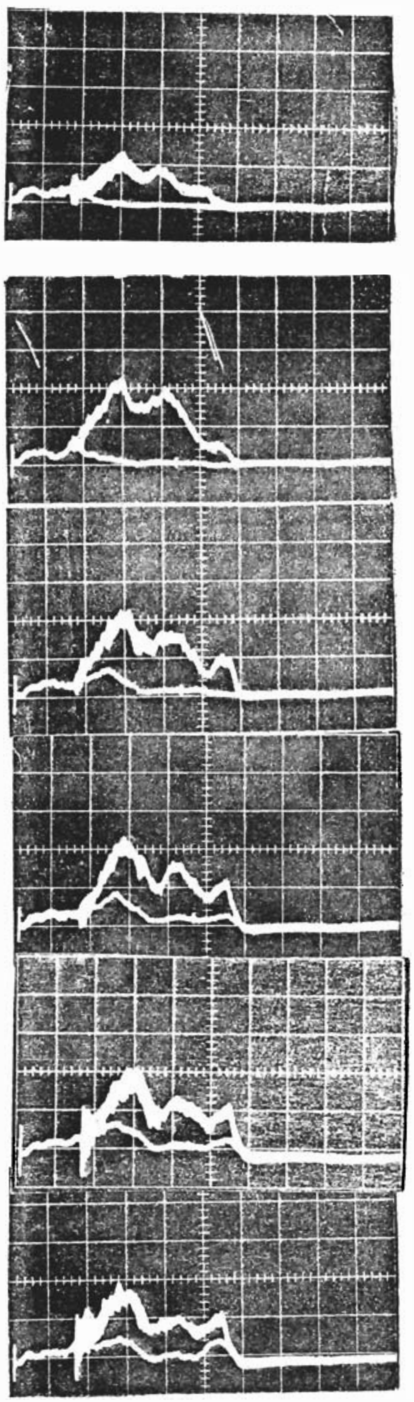

B_T= 2.3 KG

B_T= 2.9KG

B_T= 3.4 KG

B_T= 4 KG

B_T= 4.6 KG

B_T= 5.1 KG

1 MS/ DIV RF ON 1.5 TO 2.5 MS

Figure 10